International Conference on Space Optics—ICSO 2022

Dubrovnik, Croatia

3–7 October 2022

Edited by Kyriaki Minoglou, Nikos Karafolas, and Bruno Cugny,

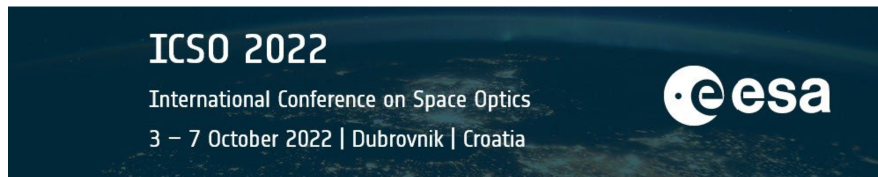

III-V based high-performance photodetectors in the non-visible regime – from UV to IR

International Conference on Space Optics — ICSO 2022, edited by Kyriaki Minoglou, Nikos Karafolas,
Bruno Cugny, Proc. of SPIE Vol. 12777, 127772F · © 2023 ESA and CNES · 0277-786X · doi: 10.1117/12.2689983

III-V based high-performance photodetectors in the non-visible regime – from UV to IR

V. Daumer*, R. Aidam, A. Bächle, R. Driad, T. Hugger, R. Keil, L. Kirste, S. Leone, W. Luppold, C. Manz, R. Müller, J. Niemasz, T. Passow, R. Rehm, F. Rutz, T. Stadelmann, M. Wobrock, A. Wörl, Q. Yang
Fraunhofer-Institute for Applied Solid State Physics IAF, Tullastr. 72, D-79108 Freiburg, Germany

ABSTRACT

Photodetectors for the non-visible region of the electromagnetic spectrum are vital for security, defense and space as well as industrial and scientific applications. The research activities at Fraunhofer IAF contribute to Europe's non-dependence on critical components and support the European strategy for critical space technologies. A broad range of III-V material systems is developed to address the spectral region adjacent to the visible regime. For the ultraviolet (UV) spectral region, AlGaN is the material of choice with an adjustable bandgap between 3.4 and 6.0 eV, depending on the Al content, addressing the wavelength regime between 365 to 210 nm. The short-wavelength infrared (SWIR) region from 0.9 up to 3.0 µm is covered by two approaches: Lattice matched InGaAs absorber material on InP substrates for a cut-off wavelength at 1.7 µm and InGaAsSb lattice matched on GaSb substrates for 1.7 up to 3.0 µm. Through the choice of appropriate layer thickness, InAs/(In,Ga)(As,Sb) type-II superlattices (T2SLs) can be tailored to cover the wavelength range from mid- to long- up to very-long-wavelength infrared (MWIR, LWIR, VLWIR) in the spectrum of 3-15 µm.

Keywords: solar-blind UV, SWIR, MWIR, LWIR, AlGaN, InGaAs, type-II superlattice, T2SL, single photon avalanche photodiode, SPAD

1. INTRODUCTION

With the general advantage of mature process technology and large, commercially available substrates, III-V based photodetectors are of high interest for many applications. Certain windows in the non-visible regime have been dominated by III-V detectors for long, e.g., InGaAs or InSb for cut-off wavelengths of 1.7 and 5.5 µm, respectively. III-V photodetectors for other regimes between UV and (V)LWIR have meanwhile reached market maturity and start replacing the previously used material systems. In many cases they overcome intrinsic limitations while maintaining or increasing the performance. Fraunhofer IAF plays a vital role in the development of modern high-performance photodetectors based on III-V semiconductors. In the following, important achievements and recent research topics are presented.

2. PHOTODETECTORS FOR THE SOLAR-BLIND UV

A compact, lightweight and all-solid-state solution for high-performance photodetectors in the UV spectral region based on AlGaN is developed at Fraunhofer IAF. Due to its tailorable bandgap, the cut-off and cut-on wavelength could be realized by choosing the appropriate Al-content during the epitaxial growth for the absorber and filter layer, respectively. Broad band and narrow band detectors with excellent out-of-band suppression could be achieved. In particular, intrinsic solar-blind UV detectors might be realized as required for defense or space applications[1]. They exhibit a very low dark current and do not degrade, even when exposed to high UV intensities.

AlGaN-based p-i-n structures were grown by metal-organic vapor phase epitaxy on 2-inch C-plane (0001)-oriented commercial or domestic AlN-on-sapphire templates. The p-i-n structure consists of a 350 nm thick Si-doped n-type contact layer, a 180 nm thick non-intentionally doped absorption layer, and a 30 nm thick Mg-doped p-type layer. All layers exhibit an Al-content of slightly above 40%. A 70 nm thick Mg-doped p-type GaN contact layer was grown on top. This layer structure was processed into mesa-type devices by photolithography and dry chemical etching. The lithographic mask contains test diodes of 50 × 50 µm^2 size and detector arrays with 640×512 pixels at 15 µm pitch. V/Al/V/Au and Ni/Au

* volker.daumer@iaf.fraunhofer.de; phone +49 761 5159-867; fax +49 761 5159-71867; www.iaf.fraunhofer.de

metal stacks were deposited by electron-beam evaporation for n- and p-type contacts, respectively. The detector arrays were diced into individual chips and a flip-chip hybridization with a read-out integrated circuit (ROIC) was performed by an external service provider. The sapphire substrate was kept unthinned and the focal plane arrays (FPAs) have no backside antireflection coating.

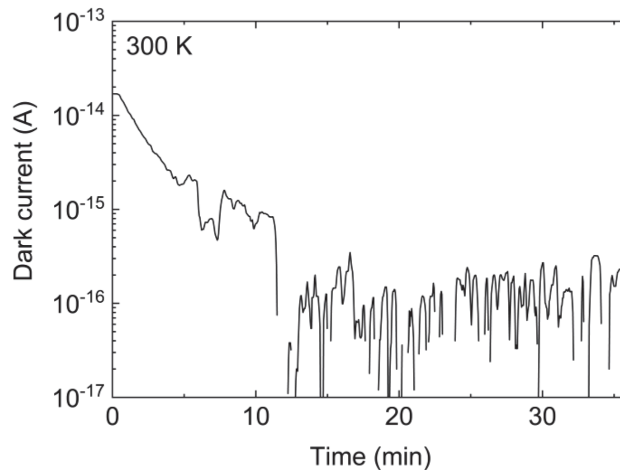

Figure 1. Dark current of a 50 × 50 μm² test diode measured at -0.2 V.

The dark current was measured using a Keysight B2987A atto-amperemeter for quadratic test diodes with a size of 50 × 50 μm². The setup was mounted inside a Faraday cage on a vibration-isolated stage to reduce the influence of the laboratory environment. The dark current was measured at a fixed reverse bias of 0.2 V versus time since the RC time constant of the AlGaN devices is huge, which makes conventional I-V characteristic measurements impractical. The result is presented in Fig. 1. Within the first approximately 10 minutes, the dark current drops by more than one order of magnitude due to the mentioned high RC time constant. Afterwards it stays clearly below 1 fA although strong fluctuations, presumably due to noise induced by the setup or lab environment, are visible. Since the active area of an FPA pixel is more than one order of magnitude smaller than that of the test diodes, the bulk dark current of an FPA pixel can be expected to be less than 0.1 fA. As the measured dark current values are setup limited, this is an upper limit for the bulk dark current of the small sized FPA pixels.

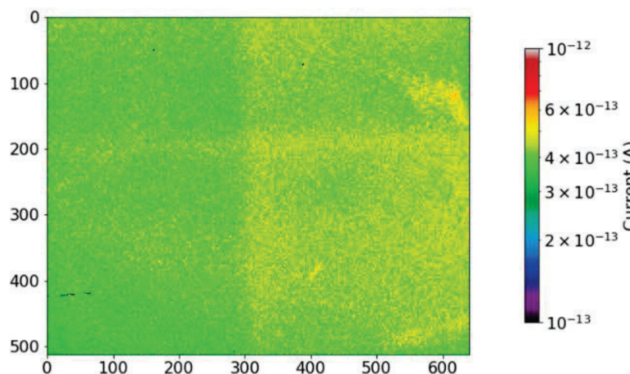

Figure 2. Map of the total pixel current for a 640×512 UV-C-FPA illuminated at 275 nm.

The FPAs were electrooptically characterized using a Pulsed Instruments System 7700 automated imaging test station to operate the ROIC. At room temperature, a dark current of a bare ROIC die of about 2 fA was determined. Hence, the dark

current of the FPA is limited by the Si-ROIC and not by the AlGaN detector matrix. The FPAs were illuminated using a high brightness, broad band plasma source coupled to a monochromator for wavelength selection. The output beam was homogenized to obtain a flat top beam profile. Figure 2 shows the map of the total pixel current for an FPA illuminated at 275 nm. The ratio of open pixels and of pixels with very high current are very low. The cross-like feature visible in the map is due to a deficiency of the homogenization optics and is not a characteristic of the FPA. The inhomogeneity of the current in the right part of the map is due to inhomogeneity in substrate transparency.

To overcome the limitations of the off-the-shelf capacitive transimpedance input amplifier (CTIA) ROIC and to access the full performance of the AlGaN-FPA, a dedicated, specifically designed low-leakage ROIC is required. The ongoing development of domestic AlN-on-sapphire template substrates aims for a non-dependence on foreign substrates and will allow for future scalability and cost-reduction.

3. PHOTODETECTORS FOR THE SWIR REGIME

The SWIR regime between 1 and 3 µm is of high interest especially for surveillance, reconnaissance, and remote sensing applications. The availability of high-power, yet eye-safe SWIR laser sources is an important asset enabling scene illumination and implementation of active imaging concepts like gated viewing (GV) or light detection and ranging (LIDAR). High-performance SWIR photodetectors are mainly realized with InGaAs absorbers that are lattice-matched to InP-substrates, providing a typical cutoff wavelength of 1.7 µm, which covers the emission lines of eye-safe laser sources at typical telecom wavelengths around 1.55 µm[2,3].

In active imaging operation, the time of flight of short laser pulses that are reflected or scattered by different obstacles in the observed scene can be utilized to determine the distance to objects of interest. Conversely, a very fast and precise trigger of a camera's frame capture with respect to the laser pulse emission can select a certain distance slice. This GV technique tremendously improves vision abilities through fog, haze, or smoke, since photons scattered by the foreground return earlier and can be excluded from the frame capture interval. The signal intensity of the returning photons at the detector, however, is extremely low and scales inversely proportional with the square of the detection range[4]. Therefore, an internal signal gain as provided by avalanche photodiodes (APDs) is of great use for GV systems.

SWIR APDs usually comprise a photon-absorbing layer and a separated multiplication layer that amplifies the current of the photo-generated carriers by the avalanche effect. Suitable high-bandgap materials for the multiplication layer are InP or InAlAs lattice-matched to InP. We use a 200-nm thin InAlAs multiplication layer because of its advantages in lower excess-noise figures[5] and a lower operating voltage that is necessary to achieve a certain gain factor. The InGaAs/InAlAs/InP heterostructures were grown by molecular beam epitaxy (MBE) on commercial n-type 3-inch InP substrate wafers in a Veeco Gen200 multi-wafer MBE machine. Our dry-etch mesa technology for processing III-V optoelectronic devices was transferred to the fabrication of the InGaAs-APD detector devices[6].

During the APD development, emphasis was put on the vertical detector design. The intermediate charge and grading layers between the InGaAs absorber and the InAlAs multiplication layer have been carefully optimized[7]. After the frontside process, InGaAs detector arrays have been hybridized with ROICs by AIM Infrarot-Module GmbH[8], followed by a backside process for substrate removal and antireflection coating.

The operating voltage range for significant gain values M, e.g., $M = 10$, could be reduced below operating bias voltages of 20 V in order to meet dedicated ROIC specifications. Focal plane arrays have been successfully integrated into gated-viewing SWIR cameras with 640×512 pixels at 15 µm pixel pitch. Fig. 3 (left) shows a section of a detector array with this spatial resolution. The avalanche operation on camera level up to a gain level of 15 was already demonstrated without defective pixel related saturation of the ROIC. The gated-viewing technique enables the acquisition of distance information alongside highly resolved images as exemplified in Fig. 3 (right) wherein the distance information is shown color-coded.

While these APDs operate in the linear mode, Geiger mode APDs operated beyond breakdown voltage address low photon flux conditions down to single photon sensitivity as required, e.g., for LIDAR applications or quantum key distribution. For this purpose, further investigations are carried out regarding InP as multiplication layer in order to design InGaAs/InP single photon avalanche detectors (SPADs), which are proven to enable stable operation conditions beyond breakdown voltage. One focus herein lies on the development of a dedicate diffusion process to form zinc doped p-type contacts using planar process technology.

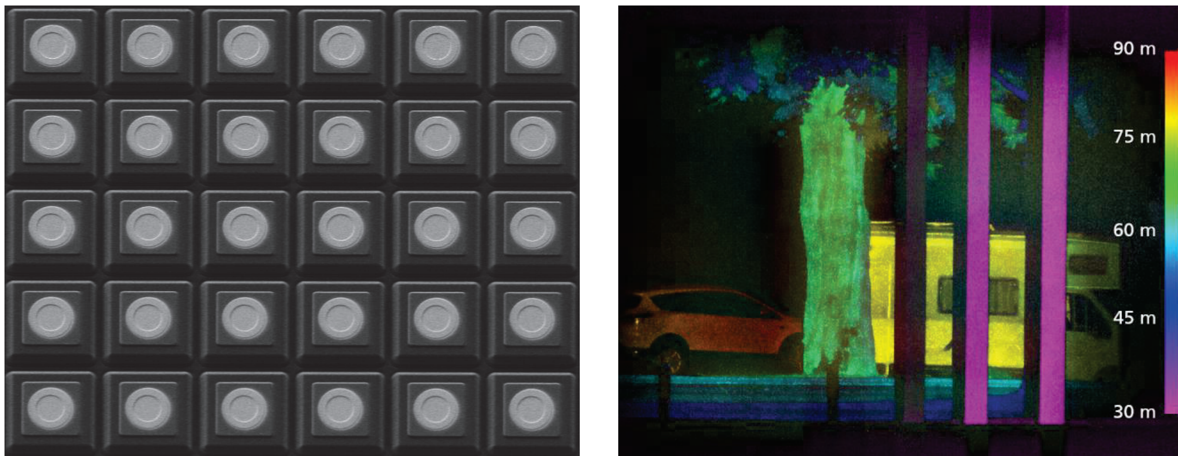

Figure 3. SEM section of a detector array with 640×512 pixels at 15 µm pitch (left) and a color-coded image depicting distance information taken by a gated-viewing SWIR camera based on mesa-processed APD arrays (right).

For cutoff wavelengths beyond 1.7 µm, InGaAs cannot be grown lattice-matched on InP. The inevitable layer strain results in high dislocation densities and, hence, limited detector performance and yield. InGaAsSb lattice-matched to GaSb is a viable alternative that is currently under investigation for room temperature operation with a heterojunction approach. Thus, the possibility to cover the whole SWIR spectral range with high-performance detector materials and advanced detector concepts will be given.

4. PHOTODETECTORS FOR THE THERMAL INFRARED

For the thermal infrared covering mid- to long- up to very-long-wavelength infrared (MWIR, LWIR, VLWIR) in the range of 3-15 µm, type-II superlattice (T2SL) infrared detectors are developed. InAs/GaSb or InAs/InAsSb T2SLs with their respective advantages are employed with respect to particular requirements, operating from cryogenic close to room temperature. Fraunhofer IAF played a vital role in the development of T2SL technology right from the start. Fundamental studies in the mid-1990s were followed by the first demonstration of two-dimensional detector arrays, leading to the first military procurement program based on T2SL detector arrays worldwide. Recent developments are driven by enhanced functionality, increased spatial resolution and a reduction of size, weight, power and costs (SWaP-C).

4.1 Mono- and bi-spectral detectors for the MWIR regime

To reduce the false alarm rate in modern missile approach warning systems, e.g., for airborne platforms, a bi-spectral T2SL detector for the MWIR has been developed. Two co-located back-to-back photodiodes with two different bandgaps, which are engineered to detect the radiation corresponding to the isolated asymmetric stretching mode of the CO_2 molecule around 4.25 µm are read out simultaneously to discriminate hot CO_2 from, e.g., a missile plume against a broad IR background with sun reflections and clutter. In more detail, this pioneering T2SL detector array consists of two times 384×288 p-i-n homojunction diodes, sensitive in the range of 3-4 µm and 4-5 µm, respectively. We have established the complete value chain for T2SL detector array fabrication in cooperation with industrial partners. Fraunhofer IAF provides design and modelling of complex heterostructures, epitaxial growth as well as front- and backside processing. These dual-color detector arrays are integrated in the self-protection system of a modern military transport aircraft at TRL9.

Early T2SL detector arrays were based on homojunction diodes and operated at around 77 K. Novel device concepts allow for substantial reduction of the dark current. Thus, the same detector performance can be achieved at significantly higher operating temperature. The reduced demand for detector cooling can be provided by smaller and cheaper coolers with extended lifetime. Several years ago, we developed InAs/GaSb T2SL heterojunction devices for the MWIR regime and employed the inherent design flexibility of the InAs/GaSb T2SLs to design a conduction band matched heterojunction device. It comprises an absorber layer with a cut-off wavelength around 5 µm and a barrier layer with an increased bandgap. This band lineup assures an unimpeded photosignal whereas the dark current is strongly suppressed. In fact, the dark

current density of the heterojunction device was more than 100 times lower than that of comparable homojunction device at 77 K [9]. Hence, this change of the device concept enabled an increase of the operating temperature by about 20 K without losing performance.

A different approach is the so-called nBn device architecture[10], consisting of a narrow-gap n-type absorber layer, a high-gap barrier (B) layer matched to the valence band and a narrow-gap n-type contact layer. As there is no depletion region in a narrow-gap layer, space-charge generation-recombination dark currents due to Shockley-Read-Hall processes are efficiently eliminated and do not limit the device performance. Furthermore, the barrier suppresses the surface leakage currents as well, due to the fact, that especially InAs-containing semiconductors are n-type on the surface. This leads to a simplified surface passivation. We have realized nBn detectors based on InAs/InAsSb T2SLs for absorber and contact layer and an AlAsSb barrier layer. All layers have been grown nearly lattice matched on GaSb substrates by MBE. Whereas the InAs/InAsSb T2SL is intrinsically n-type without external doping, the AlAsSb layer was slightly p-type doped with beryllium. Square mesa diodes with variable sizes between (60 µm)² and (350 µm)² have been fabricated. The result of the temperature-dependent dark current characterization of a test-diode with a size of (100 µm)² is presented in Fig. 4. Dark current densities have been measured from 97 K up to room temperature. The inset shows the schematic band diagram of the detector with aligned valence bands and the substantial band offset in the conduction band blocking the flow of majority carriers, i.e., electrons.

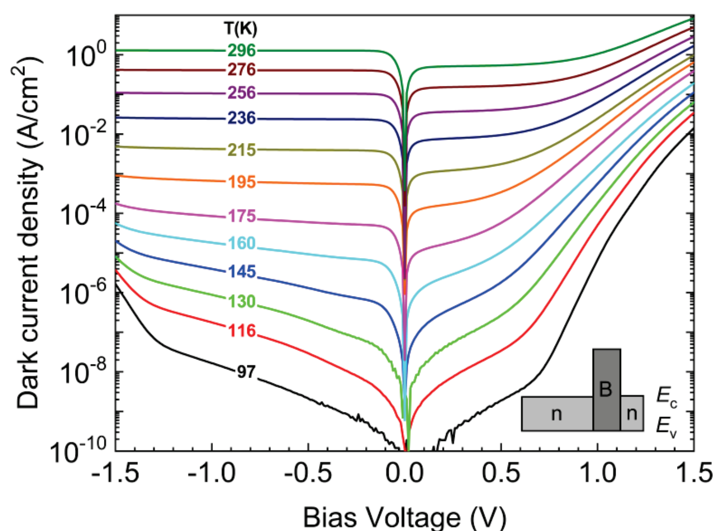

Figure 4. Dark current density as a function of the applied bias voltage, measured in the temperature range from 97 K up to room temperature. The inset shows the schematic band diagram of the nBn detector with a matching valence band energy (E_v) and a substantial offset of the conduction band energy (E_c) between absorber and the electron-blocking barrier.

The measured dark current densities are lower than the findings of a reference publication[11] due to a slightly reduced cut-off wavelength. For a meaningful comparison corrected for this deficiency, the dark current density that was measured at bias voltage of -0.2 V is plotted as a function of the inverse temperature and inverse cut-off wavelength in Fig 5. The dark current is diffusion-limited above 120 K. The device shows comparable performance to international state-of-the-art gallium-free MWIR nBn detectors[11,12]. Thus, our InAs/InAsSb T2SLs are most suitable for MWIR detector arrays with high operating temperature (HOT).

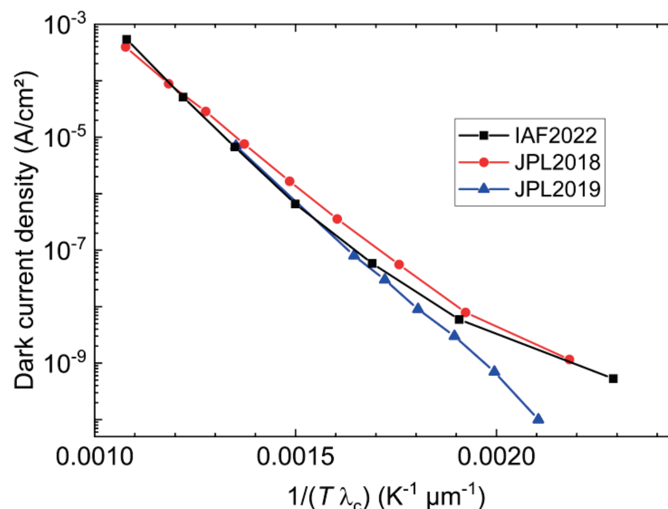

Figure 5. Dark current density as a function of the inverse temperature and inverse cut-off wavelength in comparison with recent data published by NASA Jet Propulsion Laboratory (JPL)[11,12].

Furthermore, Fraunhofer IAF contributes to the recently started collaborative ESA project "High performance T2SL infrared detectors". We will use our industry-compatible MBE process technology to supply T2SL epitaxial wafers for the fabrication of large format MWIR arrays. The project will establish a European supply chain for T2SL FPAs including design, growth, front- and backside processing as well as ROIC design and fabrication.

4.2 LWIR regime and dual-band (MWIR/LWIR) detectors

Several years ago, we have demonstrated Europe's first T2SL imager for the LWIR with 640×512 pixels at a pitch of 15 µm[13]. This device has been realized employing a heterojunction concept based on InAs/GaSb superlattices. A unipolar barrier with different composition and higher bandgap is modelled and implemented same as described for the MWIR heterojunction above. Low temperature characterization of the dark current density reveals the capability for e.g., earth observation, in comparison with HgCdTe detectors[14]. Additional advantages are higher uniformity, better temporal stability and higher operability. Furthermore, due to the mature III-V technology and available large substrates (up to 6") T2SL FPAs excel in producibility, scalability, and affordability. The successful demonstration of a LWIR imager was amongst others key for the entry into the development of MWIR/LWIR dual-band detectors. In an ongoing research project, we develop T2SL-based dual-band detectors. The layer structure for the 1280×1024 FPA with 12 µm pitch is grown on 4" GaSb substrates. It consists of two bias selectable back-to-back diodes implementing a heterojunction barrier for both bands. To avoid crosstalk between the individual pixels and to achieve a good modulation transfer function (MTF), the pixels are fully separated by mesa trenches. The large epitaxial layer thickness requires high aspect ratio trenches to maintain a high fill factor. We have realized trench widths about 2 µm on top of the structure, which assures separated pixels over the whole 4-inch wafer with a reasonable process window for an industry-compatible fabrication. A section of such a FPA after mesa etching is shown in the SEM image in Fig. 6.

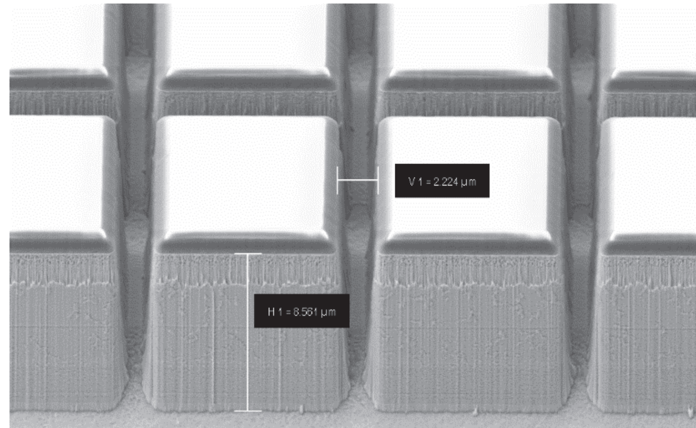

Figure 6. SEM image of a section of the 1280×1024 dual-band FPA with 12 µm pitch. The etch depth is 8.6 µm and the width at the top of the T2SL is 2.2 µm.

First test devices have been characterized at liquid nitrogen temperature. The dark current density as a function of the applied bias voltage is plotted in Fig. 7. The intended behavior can be observed: Applying a negative bias voltage addresses the MWIR diode, a positive bias voltage the LWIR device. The corresponding photoluminescence peaks as a measure of the cut-off wavelength, determined on a reference sample (not shown), are at 4.9 µm and 11.3 µm, respectively. Fine tuning of the individual layers and process optimization are the core topics of the ongoing research project.

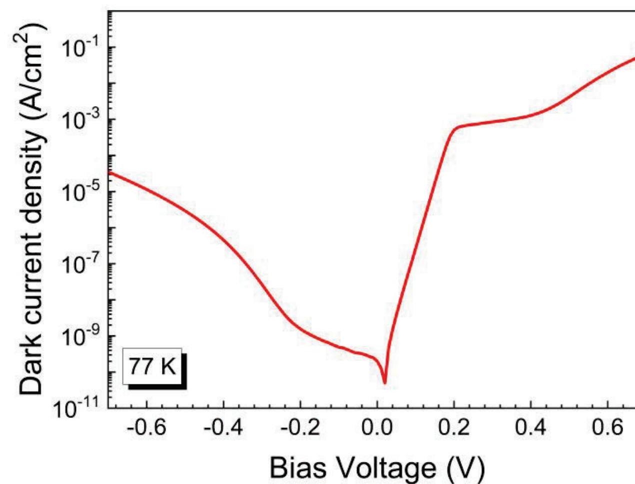

Figure 7. Dark current density as a function of the applied bias voltage, measured on a dual-band test device at 77 K. The negative bias voltage addresses the MWIR diode, the positive bias voltage the LWIR diode.

For widespread commercial applications, that require high performance at operating temperatures accessible by thermo-electric cooling (~180 – 300 K), we have developed LWIR T2SLs with metamorphic buffer layers on GaAs substrates[15]. Together with our industrial partner, we have realized single-element detectors with performance comparable to HgCdTe. In the near future, HgCdTe detectors might be excluded for widespread commercial applications in the European Union due to the RoHS (Restriction of Hazardous Substances) directive. Hence, T2SL detectors are a viable alternative here, too.

5. SUMMARY

Fraunhofer IAF is one of the leading research centers for III-V semiconductors in Europe. High-performance photodetectors for the spectral region adjacent to the visible regime are developed, employing a broad range of III-V material systems. Recent achievements from UV to IR have been presented that can overcome limitations of previously used materials. To provide an application oriented and industry-compatible photodetector technology, we have established the complete chain for detector array fabrication including design and modelling, epitaxial growth, as well as front- and backside processing.

6. ACKNOWLEDGMENTS

The authors would like to acknowledge the contributions of the Fraunhofer IAF staff for epitaxy, device processing and characterization. The support by the German Federal Ministry of Defence and the Bundeswehr Technical Center WTD81 under various contracts is gratefully acknowledged.

REFERENCES

[1] Rehm, R., Driad, R., Kirste, L., Leone, S., Passow, T., Rutz, F., Watschke, L. and Zibold, A., “Toward AlGaN Focal Plane Arrays for Solar-Blind Ultraviolet Detection”, Phys. Status Solidi A 2019, 1900769 (2019).

[2] Vollmerhausen, R. H. and Maurer, T., “Night illumination in the visible, NIR, and SWIR spectral bands,“ Proceedings of SPIE 5076, 60 (2003).

[3] DIN EN 60825-1, “Safety of Laser Products – Part 1: Equipment Classification and Requirements (IEC 60825-1:2014)”, (2022).

[4] Wandinger, U., “Introduction to Lidar”, Springer, New York, NY, p. 1–18 (2005).

[5] Saleh, M. A., Hayat, M. M., Sotirelis, P. P., Holmes, A. L., Campbell, J. C., Saleh, B. and Teich, M. C., “Impact-ionization and noise characteristics of thin III-V avalanche photodiodes,“ IEEE Trans. Electron Devices 48(12), 2722–2731 (2001).

[6] Rutz, F., Kleinow, P., Aidam, R., Bronner, W., Stolch, L., Benecke, M., Sieck, A. and Rehm, R., “SWIR detectors for low photon fluxes,“ Proceedings of SPIE 9974, 99740G (2016).

[7] Kleinow, P., Rutz, F., Aidam, R., Bronner, W., Heussen, H. and Walther, M., “Charge-layer design considerations in SAGCM InGaAs/InAlAs avalanche photodiodes,“ Phys. Status Solidi A 213(4), 925–929 (2016).

[8] Sieck, A., Benecke, M., Eich, D., Oelmaier, R., Wendler, J. and Figgemeier, H., “Short-Wave Infrared HgCdTe Electron Avalanche Photodiodes for Gated Viewing,“ Journal of Electronic Materials 47(10), 5705–5714 (2018).

[9] Schmidt, J., Rutz, F., Woerl, A., Daumer, V. and Rehm, R., “Low dark current in mid-infrared type-II superlattice heterojunction photodiodes,“ Infrared Physics & Technology 85, 378–381 (2017).

[10] Maimon, S, and Wicks, G., “nBn detector, an infrared detector with reduced dark current and higher operating temperature”, Appl. Phys. Lett., 89, 151109 (2006).

[11] Ting, D. Z., Soibel, A., Khoshakhlagh, A., Rafol, B., Keo, S. A., Höglund, L., Fisher, A. M., Luong, E. M. and Gunapala, S. D., “Mid-wavelength high operating temperature barrier infrared detector and focal plane array,“ Appl. Phys. Lett. 113(2), 21101 (2018).

[12] Soibel, A., Ting, D. Z., Rafol, B., Fisher, A. M., Keo, S. A., Khoshakhlagh, A. and Gunapala, S. D., “Mid-wavelength infrared InAsSb/InAs nBn detectors and FPAs with very low dark current density,“ Appl. Phys. Lett. 114(16), 161103 (2019).

[13] Rehm, R., Daumer, V., Hugger, T., Kohn, N., Luppold, W., Mueller, R., Niemasz, J., Schmidt, J., Rutz, F., Stadelmann, T., Wauro, M. and Woerl, A., “Type-II Superlattice Infrared Detector Technology at Fraunhofer IAF,“ Proceedings of SPIE 9819, 98190X (2016).

[14] Daumer, V., Rutz, F., Wörl, A., Niemasz, J., Müller, R., Stadelmann, T. and Rehm, R., “Type-II superlattices: a promising material for space applications“, Proceedings of SPIE 11180, 111806J-2 (2018).

[15] Müller, R., Gramich, V., Wauro, M., Niemasz, J., Kirste, L., Daumer, V., Janaszek, A., Jureńczyk, J. and Rehm, R., “High operating temperature InAs/GaSb type-II superlattice detectors on GaAs substrate for the long wavelength infrared,“ Infrared Physics & Technology 96, 141–144 (2019).